Supplementary Information

Rui-Chun Xiao[1], Yang Gao[2,*], Hua Jiang[3], Wei Gan[1], Changjin Zhang[1,4], Hui Li[1,*]

[1]*Institute of Physical Science and Information Technology and Information Materials and Intelligent Sensing Laboratory of Anhui Province, Anhui University, Hefei 230601, China*

[2]*Department of Physics, University of Science and Technology of China, Hefei 230026, China*

[3]*School of Physical Science and Technology, Soochow University, Suzhou 215006, China*

[4]*High Magnetic Field Laboratory, Chinese Academy of Sciences, Hefei 230031, China*

Email: ygao87@ustc.edu.cn (Y. G.), huili@ahu.edu.cn (H. L.)

Supplementary Note 1: Symmetry analysis of bilayer materials with interlayer sliding using *abstract bilayer crystal model*

As stated in the main text, the non-ferroelectric monolayer materials always belong to the following two cases:

1. Monolayer has inversion symmetry but no horizontal mirror symmetry, including transition-metal dichalcogenides and dihalides in $1T$ phase [short for $1T$-MX_2, such as CdI_2 and PtS_2, **Supplementary Figure 1**(a)], transition-metal dichalcogenides in $1T$' phase [short for $1T$'-MX_2, such as $MoTe_2$, WTe_2, and ZrI_2, **Supplementary Figure 1**(b)], and metal trihalide [short for MX_3, such as BiI_3 and CrI_3, **Supplementary Figure** 1(c)];

2. Monolayer has horizontal mirror symmetry but no inversion symmetry, including BN [**Supplementary Figure 2**(a)], transition-metal dichalcogenides in $1H$ phase [short for $1H$-MX_2, such as MoS_2, $MoSe_2$, WS_2 and WSe_2, **Supplementary Figure 2**(b)], and post-transition metal chalcogenides [short for MX, such InSe, GaSe and GaS, **Supplementary Figure 2**(c)].
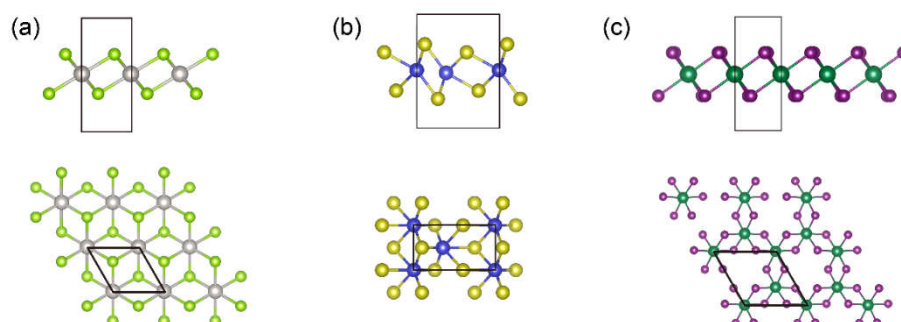
Supplementary Figure 1. Crystal structure of monolayer of (a) $1T$-MX_2, (b)$1T$'-MX_2, and (c) MX_3
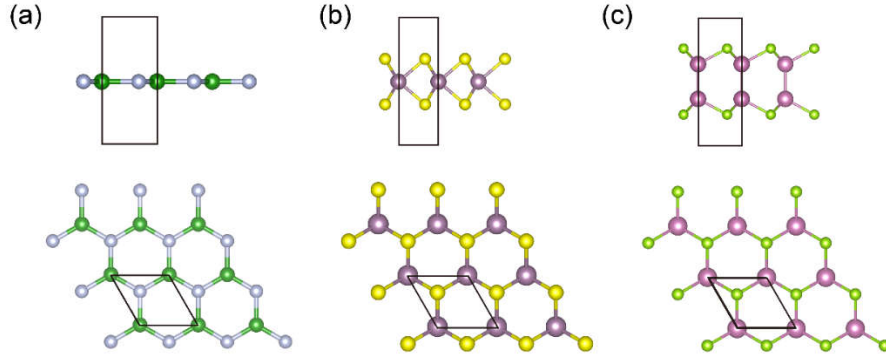
Supplementary Figure 2. Crystal structure of monolayer of (a) BN, (b) $1H$-MX$_2$, and (c) MX

In each case, the stacking way of the bilayer can be further divided into two subcases (A/A or A/B, where A or B is the crystal structure, and $B = \widehat{C}_{2z} A$).

The bilayer materials with interlayer sliding can be described with an *abstract bilayer crystal model* (as shown in **Supplementary Figure 3**) by:

$$[(A,+\mathbf{r}_{//}),(B,-\mathbf{r}_{//})], \tag{1}$$

where the parentheses $(A,+\mathbf{r}_{//})$ and $(B,-\mathbf{r}_{//})$ represent the states of the first (top) and second (button) layers respectively, where the A or B represents the crystal structure of the monolayer and $\mathbf{r}_{//}$ represents the in-plane sliding vector.
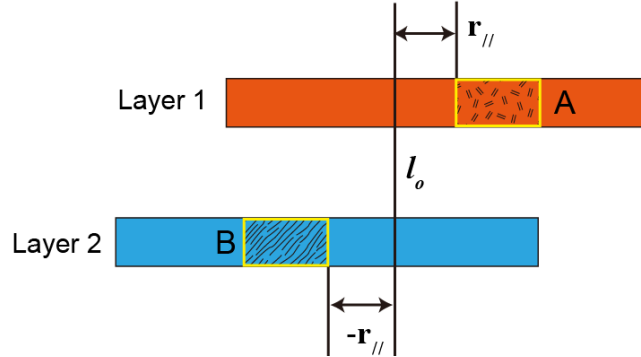

Supplementary Figure 3. Schematic of abstract bilayer crystal model. The yellow rectangles denote the unit cells, and line l_o is the original line.

In the interlayer-sliding motion, atoms in each monolayer do not move relative to themselves, so the symmetry of each layer does not change. The interlayer-sliding vector in Eq. (1) is a random number that does not equal the integral or half-integral lattice vector, so the in-plane C_2 symmetry is broken in the bilayer system. In the following, we analyze the symmetries of the bilayer materials with interlayer sliding, specifically the inversion $\widehat{I}$ and mirror $\widehat{M}_{xy}$ symmetry. In the following, we analyze the symmetry of the four cases in Table I the main text with the abstract bilayer crystal model.

Case 1: Monolayer with inversion symmetry without M_{xy} symmetry

Case 1a: A/A stacking
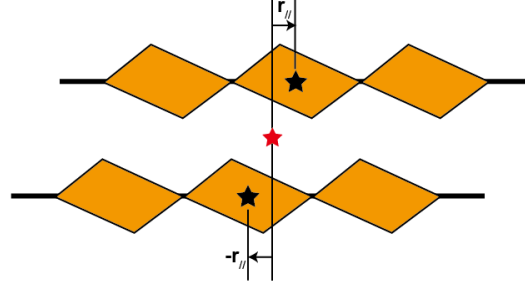
Supplementary Figure 4. 2D bilayer system stacking by Case 1a. The quadrilateral means abstract unit cell of the monolayer, and star means the inversion symmetry.

In this case, the bilayer materials are composed of two identical monolayers which both have the inversion symmetry, as shown in **Supplementary Figure 4**. According to the definition of Eq. (1), the bilayer crystal structure can be written as

$$S_+ : [(A, +\mathbf{r}_{//}), (A, -\mathbf{r}_{//})]. \tag{2}$$

Similarly, the bilayer with the opposite interlayer-sliding direction can be described as

$$S_- : [(A, -\mathbf{r}_{//}), (A, +\mathbf{r}_{//})]. \tag{3}$$

Now, we perform inversion operation $\hat{I}$ (in the middle of the bilayer and at the original axis) to the bilayer with S_+ state,

$$
\begin{aligned}
\hat{I}S_+ &= \hat{I}[(A, +\mathbf{r}_{//}), (A, -\mathbf{r}_{//})] \\
&= [\hat{I}(A, -\mathbf{r}_{//}), \hat{I}(A, +\mathbf{r}_{//})] \\
&= \left[\left(\hat{I}A, \hat{I}(-\mathbf{r}_{//}) \right), \left(\hat{I}A, \hat{I}(+\mathbf{r}_{//}) \right) \right] \\
&= [(A, +\mathbf{r}_{//}), (A, -\mathbf{r}_{//})] \\
&= S_+.
\end{aligned}
\tag{4}
$$

The formula at the second line runs because the inversion $\hat{I}$ operator between the two layers switches the first layer and the second layer. The formula at the fourth line holds because each monolayer is invariant under the inversion operator: $\hat{I}A = A$, and the sliding vector $\mathbf{r}_{//}$ reverse under the inversion operator. Therefore, the S_+ state is invariant under the inversion symmetry.

Now, we perform mirror operation $\widehat{M}_{xy}$ to S_+ state:

$$
\begin{aligned}
\widehat{M}_{xy}S_+ &= \widehat{M}_{xy}[(A, +\mathbf{r}_{//}), (A, -\mathbf{r}_{//})] \\
&= [\widehat{M}_{xy}(A, -\mathbf{r}_{//}), \widehat{M}_{xy}(A, +\mathbf{r}_{//})] \\
&= \left[\left(\widehat{M}_{xy}A, \widehat{M}_{xy}(-\mathbf{r}_{//}) \right), \left(\widehat{M}_{xy}A, \widehat{M}_{xy}(+\mathbf{r}_{//}) \right) \right] \\
&= [(B, -\mathbf{r}_{//}), (B, +\mathbf{r}_{//})].
\end{aligned}
\tag{5}
$$

Because the monolayers have no $\widehat{M}_{xy}$ symmetry, the monolayer crystal structure changes from A to B, therefore the bilayer also has no $\widehat{M}_{xy}$ symmetry.

In all, under the inversion operator $\hat{I}$, S_+ changes into itself whatever $\mathbf{r}_{//}$, so this kind of bilayer has inversion symmetry and cannot process ferroelectricity.

Case 1b: A/B stacking
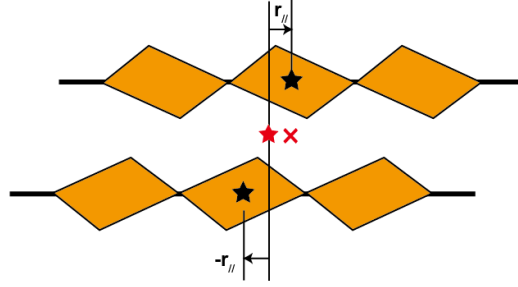
Supplementary Figure 5. 2D bilayer material stacking by Case 1b.

In this case, each monolayer is related to each other by $\widehat{C}_{2z}$ operator, as shown in **Supplementary Figure 5** (A/B stacking). The two opposite sliding states can be described as

$$\begin{cases} S_+ : [(A, +\mathbf{r}_{//}), (B, -\mathbf{r}_{//})], \\ S_- : [(A, -\mathbf{r}_{//}), (B, +\mathbf{r}_{//})], \end{cases} \tag{6}$$

where

$$\begin{cases} \hat{I}A = A, \\ \hat{I}B = B, \end{cases} \tag{7}$$

and each monolayer crystal structure is switched by $\widehat{C}_{2z}$ symmetry:

$$\begin{cases} \widehat{C}_{2z}A = B, \\ \widehat{C}_{2z}B = A. \end{cases} \tag{8}$$

For a system with inversion symmetry $\hat{I}$, $\widehat{M}_{xy}$ and $\widehat{C}_{2z}$ operators are equivalent, because $\hat{I}\widehat{C}_{2z} = \widehat{M}_{xy}$. Therefore, the monolayer crystal structure is also switched under the $\widehat{M}_{xy}$ operator:

$$\begin{cases} \widehat{M}_{xy}A = B, \\ \widehat{M}_{xy}B = A. \end{cases} \tag{9}$$

Now, we perform inversion operation $\hat{I}$ to the S_+ state,

$$\begin{aligned}
\hat{I}S_+ &= \hat{I}[(A,+\mathbf{r}_{//}),(B,-\mathbf{r}_{//})] \\
&= \left[\hat{I}(B,-\mathbf{r}_{//}),\hat{I}(A,+\mathbf{r}_{//})\right] \\
&= [(B,+\mathbf{r}_{//}),(A,-\mathbf{r}_{//})].
\end{aligned} \tag{10}$$

$\hat{I}S_+ \neq S_+$, so bilayer S_+ does not have the inversion symmetry whatever $\mathbf{r}_{//}$. Besides, $\hat{I}S_+ \neq S_-$, therefore the two opposite interlayer-sliding states are not connected by inversion operation.

Performing $\widehat{M}_{xy}$ operation to the S_+ state,

$$\begin{aligned}
\widehat{M}_{xy}S_+ &= \widehat{M}_{xy}[(A,+\mathbf{r}_{//}),(B,-\mathbf{r}_{//})] \\
&= \left[\widehat{M}_{xy}(B,-\mathbf{r}_{//}),\widehat{M}_{xy}(A,+\mathbf{r}_{//})\right] \\
&= [(A,-\mathbf{r}_{//}),(B,+\mathbf{r}_{//})] \\
&= S_-.
\end{aligned} \tag{11}$$

The formula at the second line holds because the $\widehat{M}_{xy}$ operator between the two layers will switch the first layer and the second layer. The formula after the third line runs because the monolayer crystal types switch under $\widehat{M}_{xy}$ [Eq. (9)], and $\mathbf{r}_{//}$ is invariant under $\widehat{M}_{xy}$. Therefore, under the $\widehat{M}_{xy}$ operation, S_+ cannot transform into itself but convert to the S_- state. Besides, the bilayer has the $\widehat{M}_{xy}$ symmetry if $\mathbf{r}_{//} = 0$.

To sum up, the bilayer crystal structure in Case 1b does not have both inversion and $\widehat{M}_{xy}$ symmetry, but the two opposite interlayer-sliding states are connected by $\widehat{M}_{xy}$ symmetry.

Case 2 Monolayer without inversion symmetry but has the M_{xy} symmetry

Case 2a: A/A stacking
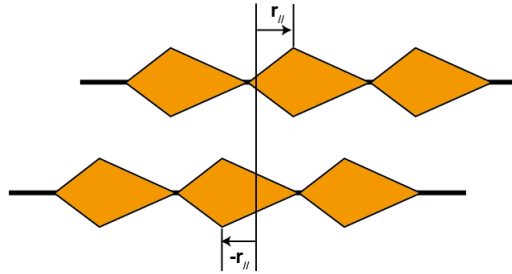
Supplementary Figure 6. 2D bilayer material stacking by Case 2a.

In this case, the bilayer material is composed of two identical monolayers without inversion symmetry but with the $\widehat{M}_{xy}$ symmetry, as shown in **Supplementary Figure 6**. The two opposite interlayer-sliding states of this case can be described as

$$\begin{cases} S_+ : [(A,+\mathbf{r}_{//}),(A,-\mathbf{r}_{//})], \\ S_- : [(A,-\mathbf{r}_{//}),(A,+\mathbf{r}_{//})]. \end{cases} \tag{12}$$

The monolayer crystal structure is invariant under the $\widehat{M}_{xy}$ operation: $\widehat{M}_{xy}A = A$.

Performing $\hat{I}$ operation to the S_+ state, we will get

$$\begin{aligned} \hat{I}S_+ &= \hat{I}[(A,+\mathbf{r}_{//}),(A,-\mathbf{r}_{//})] \\ &= \left[\hat{I}(A,-\mathbf{r}_{//}),\hat{I}(A,+\mathbf{r}_{//}) \right] \\ &= [(B,+\mathbf{r}_{//}),(B,-\mathbf{r}_{//})], \end{aligned} \tag{13}$$

where the monolayer has no inversion symmetry, and A transforms into B under $\hat{I}$. We find $\hat{I}S_+ \neq S_+$, and $\hat{I}S_+ \neq S_-$. Therefore, S_+ does not have the inversion symmetry, and the two opposite interlayer-sliding states are not related to each other by the inversion operation either.

We perform the $\widehat{M}_{xy}$ operator to S_+ state,

$$\begin{aligned} \widehat{M}_{xy}S_+ &= \widehat{M}_{xy}[(A,+\mathbf{r}_{//}),(A,-\mathbf{r}_{//})] \\ &= \left[\widehat{M}_{xy}(A,-\mathbf{r}_{//}),\widehat{M}_{xy}(A,+\mathbf{r}_{//}) \right] \\ &= [(A,-\mathbf{r}_{//}),(A,+\mathbf{r}_{//})] \\ &= S_-. \end{aligned} \tag{14}$$

Therefore, S_+ has no $\widehat{M}_{xy}$ symmetry if $\mathbf{r}_{//} \neq 0$, but S_+ can convert to S_- by $\widehat{M}_{xy}$.

In summary, the bilayer 2D materials in Case 2a do not have both inversion $\hat{I}$ and $\widehat{M}_{xy}$ symmetry, but the two opposite interlayer-sliding states are connected by $\widehat{M}_{xy}$ operation.

Case 2b A/B stacking

★ Bilayer inversion center
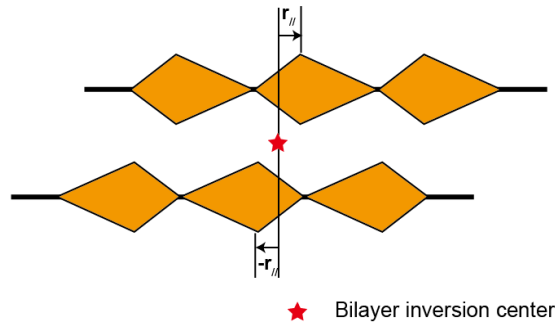
Supplementary Figure 7. 2D bilayer material stacking by Case 2b

In this case, the bilayer is constituted by two 180°-rotated monolayers (A/B stacking), as shown in **Supplementary Figure 7**. The two opposite interlayer-sliding states of this case can be described as

$$\begin{cases} S_+ : [(A,+\mathbf{r}_{//}),(B,-\mathbf{r}_{//})], \\ S_- : [(A,-\mathbf{r}_{//}),(B,+\mathbf{r}_{//})], \end{cases} \tag{15}$$

where each layer has the $\widehat{M}_{xy}$ symmetry:

$$\begin{cases} \widehat{M}_{xy}A = A, \\ \widehat{M}_{xy}B = B. \end{cases} \tag{16}$$

and each monolayer is switched by $\widehat{C}_{2z}$ symmetry

$$\begin{cases} \widehat{C}_{2z}A = B, \\ \widehat{C}_{2z}B = A. \end{cases} \tag{17}$$

In a system with $\widehat{M}_{xy}$ symmetry, $\widehat{C}_{2z}$ and $\hat{I}$ are equivalent, because $\widehat{M}_{xy}\widehat{C}_{2z} = \hat{I}$. Therefore, the monolayer crystal types are also switched under $\hat{I}$:

$$\begin{cases} \hat{I}A = B, \\ \hat{I}B = A. \end{cases} \tag{18}$$

Performing $\hat{I}$ operation to the S_+ state,

$$\begin{aligned} \hat{I}S_+ &= \hat{I}[(A,+\mathbf{r}_{//}),(B,-\mathbf{r}_{//})] \\ &= \left[\hat{I}(B,-\mathbf{r}_{//}), \hat{I}(A,+\mathbf{r}_{//}) \right] \\ &= [(A,+\mathbf{r}_{//}),(B,-\mathbf{r}_{//})] \\ &= S_+. \end{aligned} \tag{19}$$

S_+ turns itself into itself under inversion operation whatever $\mathbf{r}_{//}$, so this structure has inversion symmetry, even though the monolayer has no inversion symmetry. Therefore, the bilayer in Case 2b cannot have ferroelectricity and BPVE.

Besides, we perform inversion operation $\widehat{M}_{xy}$ to S_+ state:

$$\begin{aligned} \widehat{M}_{xy}S_+ &= \widehat{M}_{xy}[(A,+\mathbf{r}_{//}),(B,-\mathbf{r}_{//})] \\ &= [\widehat{M}_{xy}(B,-\mathbf{r}_{//}), \widehat{M}_{xy}(A,+\mathbf{r}_{//})] \\ &= \left[\left(\widehat{M}_{xy}B, \widehat{M}_{xy}(-\mathbf{r}_{//}) \right), \left(\widehat{M}_{xy}A, \widehat{M}_{xy}(+\mathbf{r}_{//}) \right) \right] \\ &= [(B,-\mathbf{r}_{//}),(A,+\mathbf{r}_{//})] \neq S_+ \end{aligned} \tag{20}$$

Even though monolayer lattices A and B have the $\widehat{M}_{xy}$ symmetry, this kind of bilayer has no $\widehat{M}_{xy}$ symmetry.

The above four cases are summarized in Table I of the main text.

Last but not least, in real materials such as bilayer MoS$_2$, BN, InSe, GaSe (Case 2a), except the sliding vector $\mathbf{r}_{//}$, there is also a half lattice vector shift $1/2\mathbf{a}_\perp$ for the

top layer in the positive and negative ferroelectric state. $1/2\mathbf{a}_\perp$ is vertical to the interlayer-sliding direction [see Fig. 2 (a) in the main text]. The two interlayer-sliding states in Eq. (12) of Case 2a are changed into

$$\begin{cases} S_+ : [(A, +\mathbf{r}_{//} + 1/2\mathbf{a}_\perp), (A, -\mathbf{r}_{//} + 1/2\mathbf{a}_\perp)], \\ S_- : [(A, -\mathbf{r}_{//} + 1/2\mathbf{a}_\perp), (A, +\mathbf{r}_{//} + 1/2\mathbf{a}_\perp)], \end{cases} \tag{21}$$

The crystals have the translation symmetry with integer lattice vector, so we can shift the second/first layer with an integral constant vector $-\mathbf{a}_\perp$ for S_+/S_-, then

$$\begin{cases} S'_+ : [(A, +\mathbf{r}_{//} + 1/2\mathbf{a}_\perp), (A, -\mathbf{r}_{//} - 1/2\mathbf{a}_\perp)], \\ S'_- : [(A, -\mathbf{r}_{//} - 1/2\mathbf{a}_\perp), (A, +\mathbf{r}_{//} + 1/2\mathbf{a}_\perp)]. \end{cases} \tag{22}$$

Now, Eq. (22) here is equal to Eq. (12) in Case 2a.
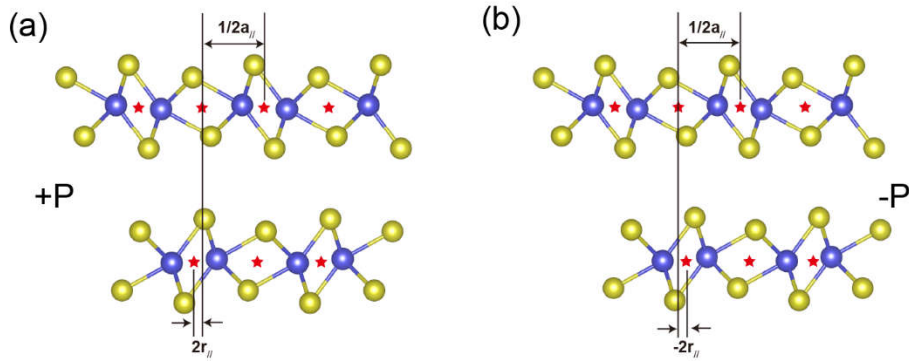
Supplementary Figure 8. Interlayer sliding of bilayer WTe$_2$ with (a) +P and (b) –P states, where $2\mathbf{r}_{//}$ means the interlayer sliding vector compared to **Supplementary Figure 5**.

For bilayer WTe$_2$ (Case 1b), except for the half lattice vector shift $1/2\mathbf{a}_\perp$ [See Fig. 3 (a) in the main text], there also is a half lattice vector interlayer shift $1/2\mathbf{a}_{//}$ that is parallel to the interlayer-sliding direction [**Supplementary Figure 8**]. The two interlayer-sliding states for bilayer WTe$_2$ are

$$\begin{cases} S_+ : [(A, +\mathbf{r}_{//} + 1/2\mathbf{a}_\perp + 1/2\mathbf{a}_{//}), (B, -\mathbf{r}_{//} + 1/2\mathbf{a}_\perp + 1/2\mathbf{a}_{//})], \\ S_- : [(A, -\mathbf{r}_{//} + 1/2\mathbf{a}_\perp + 1/2\mathbf{a}_{//}), (B, +\mathbf{r}_{//} + 1/2\mathbf{a}_\perp + 1/2\mathbf{a}_{//})], \end{cases} \tag{23}$$

Similarly, if we shift the second/first layer with $-\mathbf{a}_\perp - \mathbf{a}_{//}$ for S_+/S_-, the two new interlayer-sliding states are

$$\begin{cases} S'_+ : [(A, +\mathbf{r}_{//} + 1/2\mathbf{a}_\perp), (B, -\mathbf{r}_{//} - 1/2\mathbf{a}_\perp - 1/2\mathbf{a}_{//})], \\ S'_- : [(A, -\mathbf{r}_{//} - 1/2\mathbf{a}_\perp - 1/2\mathbf{a}_{//}), (B, +\mathbf{r}_{//} + 1/2\mathbf{a}_\perp)]. \end{cases} \tag{24}$$

Here, Eq. (24) is equal to Eq. (6) in Case 1b. Therefore, the above rule of Case 1b is also suitable to the bilayer WTe$_2$.

Supplementary Note 2: Effect model for 1D interlayer sliding

The 1D single chain in **Fig. 1** (a) of the main text is very similar to the SSH (Su-Schrieffer-Heeger) Hamiltonian model

$$\hat{H} = \varepsilon_a \sum_i \hat{a}_i^\dagger \hat{a}_i + \varepsilon_b \sum_i \hat{b}_i^\dagger \hat{b}_i + \sum_i \left(J \hat{a}_i^\dagger \hat{b}_i + J' \hat{a}_i^\dagger \hat{b}_{i-1} + h.c. \right), \qquad (25)$$

i.e.

$$H_0 = \begin{bmatrix} \varepsilon_a & T_{ab} \\ T_{ba} & \varepsilon_b \end{bmatrix}, \qquad (26)$$

where $T_{ab} = T_{ba}^* = J \exp(ik_x) + J' \exp(-ik_x)$, J and J' mean the nearest atom hopping, and ε_a and ε_b mean the onsite energies for a (anion) and b (cations) atoms.

For the bi-chain with $+P$ which considering the nearest inter-chain hopping in Fig. 1(a) of the main text, the corresponding effect model is

$$H(+P) = \begin{bmatrix} \varepsilon_a & T_{ab} & 0 & 0 \\ T_{ba} & \varepsilon_b & t_\perp & 0 \\ 0 & t_\perp & \varepsilon_a & T_{ab} \\ 0 & 0 & T_{ba} & \varepsilon_b \end{bmatrix}, \qquad (27)$$

where the basis is $\left\{ \varphi_a^\uparrow, \varphi_b^\uparrow, \varphi_a^\downarrow, \varphi_b^\downarrow \right\}$, and $t_\perp$ is the nearest hopping parameter between two chains as shown in **Supplementary Figure 9**(a). The effective model in bi-chain of $-P$ in **Fig. 1** (c) of the main text is

$$H(-P) = \begin{bmatrix} \varepsilon_a & T_{ab} & 0 & t_\perp \\ T_{ba} & \varepsilon_b & 0 & 0 \\ 0 & 0 & \varepsilon_a & T_{ab} \\ t_\perp & 0 & T_{ba} & \varepsilon_b \end{bmatrix}. \qquad (28)$$

The $H(+P)$ and $H(-P)$ are correlated by the mirror symmetry

$$\widehat{M}_z = \begin{bmatrix} 0 & I_0 \\ I_0 & 0 \end{bmatrix} = \begin{bmatrix} 0 & 0 & 1 & 0 \\ 0 & 0 & 0 & 1 \\ 1 & 0 & 0 & 0 \\ 0 & 1 & 0 & 0 \end{bmatrix} \qquad (29)$$

i.e.

$$\widehat{M}_z H(+P) \widehat{M}_z = H(-P). \qquad (30)$$

Supplementary Figure 9(b) shows the band structure of bi-chain. The in-plane and out-of-plane BPVE coefficients are shown in **Supplementary Figure 9**(c) and (d). Consistent with our symmetry analysis, the in-plane BPVE coefficients are invariant while the out-of-plane BPVE coefficients change with the ferroelectric order.
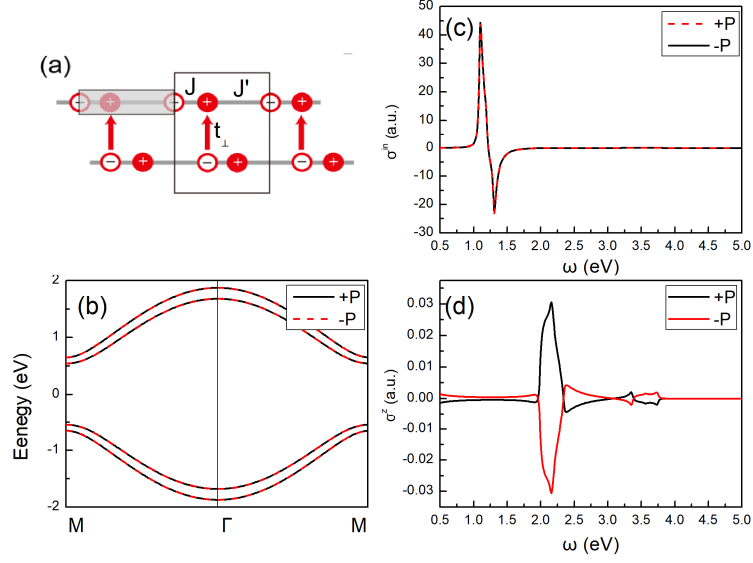
Supplementary Figure 9. (a) 1D bi-chain SSH model. (b) Band structure. (c) In-plane and (d) out-of-plane BPVE coefficients. $\varepsilon_a = -\varepsilon_b = 0.5eV$, $J = 1eV$, $J' = 0.7eV$, $t_\perp = 0.2eV$.

Supplementary Note 3: Symmetry analysis of the BPVE coefficients

Except for the symmetry requirement shown the Eq. (3) of the main text, the BPVE tensor $\left[\sigma_{bc}^a\right]_{3\times3\times3}$ elements have the subscripts-switch symmetry, *i.e.* $\sigma_{jk}^j = \sigma_{kj}^j$. Therefore, the $3\times3\times3$ σ_{bc}^a tensor can be contracted as a 3×6 matrix $\left[\sigma_{jk}^i\right]_{3\times6}$, and the elements in each row are in the sequence of σ_{xx}^i, σ_{yy}^i, σ_{zz}^i, σ_{yz}^i, σ_{xz}^i and σ_{xy}^i.

Acoordingly, BPVE tensor of bilayer ferroelectric MoS$_2$ with C$_{3v}$ symmetry is

$$\left[\sigma_{jk}^i\right]_{3\times6} = \begin{bmatrix} 0 & 0 & 0 & 0 & \sigma_{xz}^x & -\sigma_{yy}^y \\ -\sigma_{yy}^y & \sigma_{yy}^y & 0 & \sigma_{xz}^x & 0 & 0 \\ \sigma_{xx}'^z & \sigma_{xx}'^z & \sigma_{zz}^z & 0 & 0 & 0 \end{bmatrix}. \tag{31}$$

The tensor elements in red mean the in-plane BPVE coefficients, and $\sigma_{xy}^x = \sigma_{xx}^y = -\sigma_{yy}^y$, and $\sigma_{xx}^x = \sigma_{yy}^x = \sigma_{xy}^y = 0$. The elements in blue in Eq. (31) represent the out-of-plane BPVE coefficients under the normal incidence of light, and we find that $\sigma_{xx}'^z = \sigma_{yy}'^z$, and $\sigma_{xy}'^z = \sigma_{yx}'^z = 0$.

For bilayer ferroelectric WTe$_2$ with C_{1v} symmetry, the BPVE tensor is

$$\left[\sigma^i_{jk} \right]_{3\times 6} = \begin{bmatrix} 0 & 0 & 0 & 0 & \sigma^x_{xz} & \sigma^x_{xy} \\ \sigma^y_{xx} & \sigma^y_{yy} & \sigma^y_{zz} & \sigma^y_{yz} & 0 & 0 \\ \sigma'^z_{xx} & \sigma'^z_{yy} & \sigma^z_{zz} & \sigma^z_{yz} & 0 & 0 \end{bmatrix}. \tag{32}$$

Due to lower symmetry, the BPVE tensor of bilayer WTe$_2$ is more complicated than those of bilayer MoS$_2$ [Eq. (31)]. We find there are three independent in-plane BPVE coefficients σ^x_{xy}, σ^y_{xx}, σ^y_{yy}, and $\sigma^x_{xx} = \sigma^x_{yy} = \sigma^y_{xy} = 0$ due to $\widehat{M}_{yz}$ symmetry, and two independent out-of-plane BPVE coefficients σ'^z_{xx} and σ'^z_{yy} ($\sigma'^z_{xy} = \sigma'^z_{yx} = 0$) for ferroelectric bilayer WTe$_2$, which is consistent with our calculation results.

Supplementary Note 4: In-plane and out-of-plane BPVE with the polarization of light

Now, we study the in-plane and out-of-plane BPVE response with the polarization of light. For a linearly polarized light, $\mathbf{E}(\omega)$ is a vector. For the 2D material under the normal incidence of light, $\mathbf{E}(\omega)$ only has the E_x and E_y components, and

$$\begin{cases} E_x = E\cos\theta, \\ E_y = E\sin\theta, \end{cases} \tag{33}$$

where E is the magnitude of the light, and θ is the azimuthal angle relative to the x axis.

According to Eq. (31), the in-plane BPVE current of bilayer MoS$_2$ is

$$\begin{cases} j_x = -\sigma^y_{yy} E^2 \sin 2\theta, \\ j_y = -\sigma^y_{yy} E^2 \cos 2\theta. \end{cases} \tag{34}$$

If the light is the natural light that contains all-directions linearly polarized lights, θ varies from 0 to π, so the in-plane BPVE current is the sum of all the polarized light:

$$\int_0^\pi j_x = 0, \quad \int_0^\pi j_y = 0. \tag{35}$$

Therefore, the light should be linearly polarized to get the in-plane BPVE. The out-of-plane BPVE (light-induced polarization) of bilayer MoS$_2$ is

$$p_z = \left(E^2 \sigma'^z_{xx} \cos^2\theta + E^2 \sigma'^z_{yy} \sin^2\theta \right) = \sigma'^z_{xx} E^2, \tag{36}$$

because $\sigma'^z_{xx} = \sigma'^z_{yy}$, and $\sigma'^z_{xy} = \sigma'^z_{yx} = 0$. According to Eq. (36), the out-of-plane BPVE polarization is isotropic and independent of the direction of the polarization of light, as shown in Fig. 2 (f) in the main text.

Similarly, for bilayer WTe$_2$, we find in-plane BPVE current obeys

$$\begin{cases} j_x = \sigma_{xy}^x E^2 \sin 2\theta, \\ j_y = E^2 \left(\sigma_{xx}^y \cos^2 \theta + \sigma_{yy}^y \sin^2 \theta \right). \end{cases} \tag{37}$$

The in-plane BPVE only shows the $\widehat{M}_{yz}$ symmetry, as shown in the main text. Because $\sigma_{xy}'^z = \sigma_{yx}'^z = 0$, $\sigma_{xx}'^z \neq \sigma_{yy}'^z \neq 0$, the out-of-plane BPVE polarization is

$$p_z = \sigma_{xx}'^z E^2 \cos^2 \theta + \sigma_{yy}'^z E^2 \sin^2 \theta. \tag{38}$$

According to Eq. (38), the light-induced BPVE polarization is anisotropic and dependent on the direction of the polarization of light, as shown in Fig. 3 (f) in the main text.

Supplementary Note 5: In-plane and out-of-plane BVPE of MoS$_2$ with interlayer sliding displacement

To show the dependence of in-plane and out-of-plane BPVE with interlayer sliding displacement, we manually change the interlayer sliding displacement defining as a parameter ζ. $\zeta=0$ corresponds to no interlayer sliding, while $\zeta=+1/-1$ corresponds to the $+P/-P$ phase.

In-plane and out-of-plane BVPE of bilayer MoS$_2$ with ζ are shown in **Supplementary Figure 10**. The in-plane BVPE coefficient is even with interlayer sliding displacement parameter ζ, while the out-of-plane BVPE coefficient is odd with ζ. The out-of-plane BVPE vanishes when $\zeta=0$, while the in-plane BVPE still exists. The in-plane BPVE is robust with the interlayer sliding displacement ζ, while the out-of-plane BPVE is sensitive to the interlayer sliding displacement ζ.
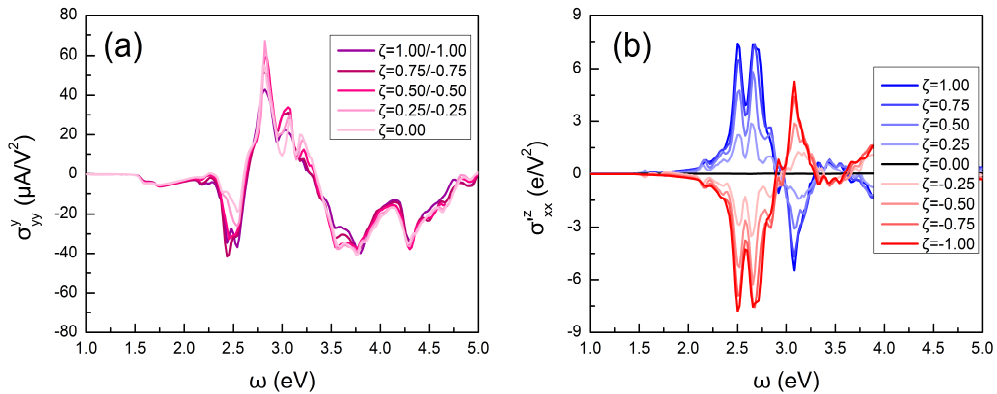

Supplementary Figure 10. (a) In-plane BVPE coefficient σ_{yy}^y and (b) out-of-plane BVPE coefficient $\sigma_{xx}'^z$ of bilayer MoS$_2$ with interlayer-sliding displacement ζ.

Supplementary Note 6: Band structures and BPVE coefficients with the choice of vdW correction

We calculated the band structures and BPVE coefficients with DFT-D2 (presented in the main text) and DFT-D3 vdW correction for bilayer MoS_2 and WTe_2. The crystal structures are relaxed accordingly. As shown in **Supplementary Figure 11** and **Supplementary Figure 12**, the band structures and BPVE coefficients depend on the vdW corrections. However, the magnitude of the out-of-plane and in-plane BPVE coefficients of two materials are basically the same, which is what we care more about.

Besides, we think the above calculation deviations mainly come from differences in crystal structure caused by structural optimization via vdW correction. We calculated the band structures and BPVE coefficients of bilayer MoS_2 with the same crystal structure but with different vdW corrections. We find that the results are almost the same, as shown in **Supplementary Figure 13**.
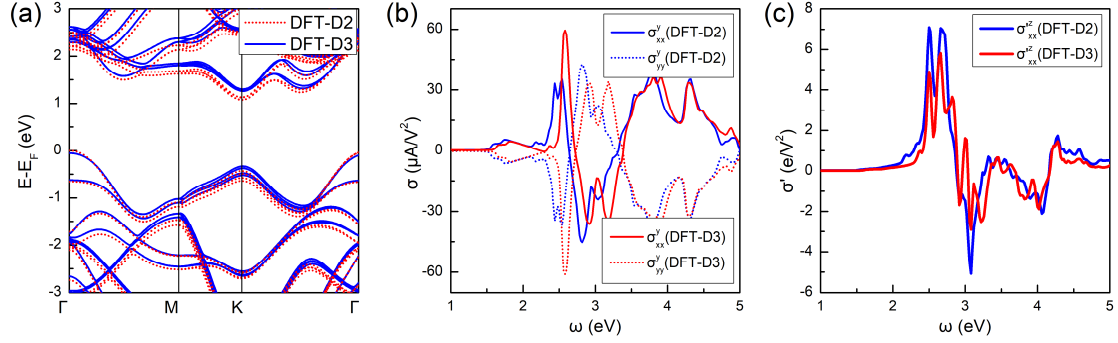
Supplementary Figure 11. (a) Band structure, (b) in-plane BPVE, and (c) out-of-plane BPVE of bilayer MoS_2 (with $+P$ phase) with the choice of vdW corrections. The crystal structure of bilayer MoS_2 is relaxed using vdW correction accordingly.
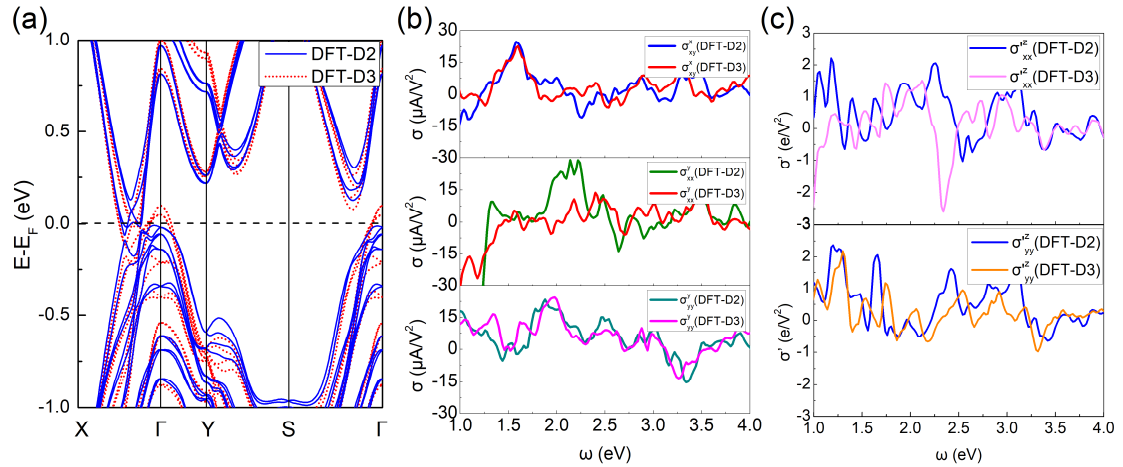
Supplementary Figure 12. (a) Band structure, (b) in-plane BPVE, and (c) out-of-plane BPVE of bilayer WTe_2 (with $+P$ phase) with the choice of vdW corrections. The crystal structure of bilayer WTe_2 is relaxed using the vdW correction accordingly.
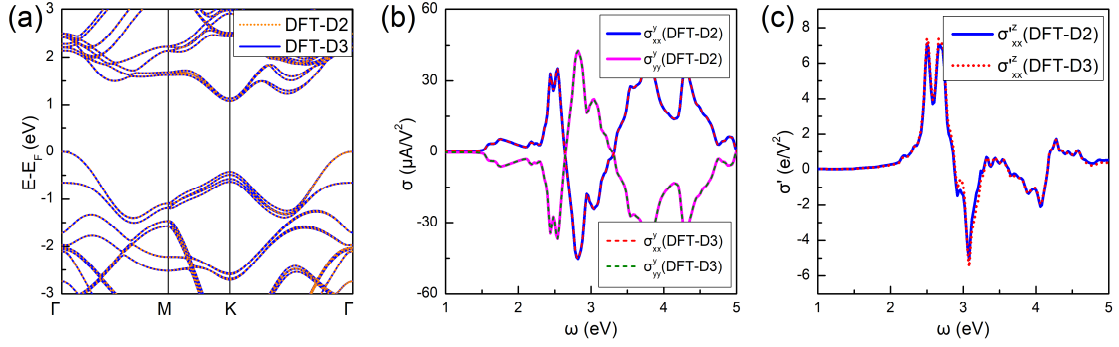
Supplementary Figure 13. (a) Band structure, (b) in-plane BPVE, and (c) out-of-plane BPVE of bilayer MoS$_2$ (with +P phase) with different vdW corrections but with the same crystal structure.
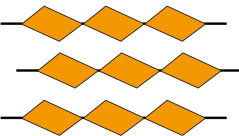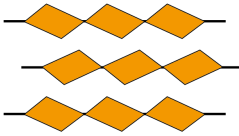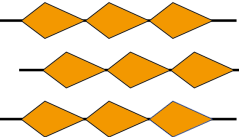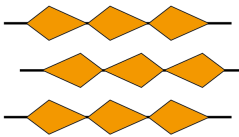

Supplementary Note 7: Symmetry of trilayer vdW materials with interlayer sliding

We can use our abstract model to analyze the symmetry of the trilayer vdW materials with interlayer sliding. We can divide them into two situations: (1) the top and bottom layer slide along the same direction relative to the middle layer, (2) the top and bottom layer slide along the opposite directions relative to the middle layer. Using a similar method as *Supplementary Note 1*, we can obtain the symmetry of trilayer interlayer-sliding ferroelectric materials which are summarized are in **Supplementary Table I** and **Supplementary Table II** respectively. The ferroelectricity and BPVE obey the following rules:
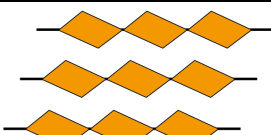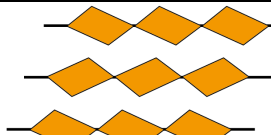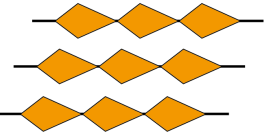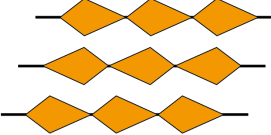
(1) For the first situation, we find that only Case 1a and Case 1b have ferroelectricity, and the two opposite ferroelectric states are related by the inversion symmetry (**Supplementary Table I**). Therefore, the in-plane and out-of-plane BPVE are both reversed with ferroelectric order in these two cases. Trilayer WTe$_2$ [*npj Comput. Mater.* 5, 119, (2019)] belongs to Case 1b here.

(2) For the second situation, we find that only Case 2a and Case 2b have ferroelectricity, and the two opposite ferroelectric states are related by the mirror symmetry (**Supplementary Table II**). Therefore, the out-of-plane BPVE reverses with ferroelectric order, while the in-plane BPVE invariant for trilayer materials with these stacking ways.

Supplementary Table I. Symmetries of trilayer vdW material with top and bottom layer sliding along the same direction.

Stacking way / Monolayer symmetry	a. A/A/A	b. A/B/A
1. $\begin{cases} \hat{I}: \quad \checkmark \\ \widehat{M}_{xy}: \quad \times \end{cases}$	Case 1a: $\begin{cases} \hat{I}: \quad \times \\ \widehat{M}_{xy}: \quad \times \\ \hat{I}S_+ = S_- \end{cases}$	Case 1b: $\begin{cases} \hat{I}: \quad \times \\ \widehat{M}_{xy}: \quad \times \\ \hat{I}S_+ = S_- \end{cases}$
2. $\begin{cases} \hat{I}: \quad \times \\ \widehat{M}_{xy}: \quad \checkmark \end{cases}$	Case 2a: $\begin{cases} \hat{I}: \quad \times \\ \widehat{M}_{xy}: \quad \checkmark \end{cases}$	Case 2b: $\begin{cases} \hat{I}: \quad \times \\ \widehat{M}_{xy}: \quad \checkmark \end{cases}$

Supplementary Table II. Symmetries of trilayer vdW material with top and bottom layer sliding along the opposite directions.

Stacking way / Monolayer symmetry	a. A/A/A	b. A/B/A
1. $\begin{cases} \hat{I}: \quad \checkmark \\ \widehat{M}_{xy}: \quad \times \end{cases}$	Case 1a: $\begin{cases} \hat{I}: \quad \checkmark \\ \widehat{M}_{xy}: \quad \times \end{cases}$	Case 1b: $\begin{cases} \hat{I}: \quad \checkmark \\ \widehat{M}_{xy}: \quad \times \end{cases}$
2. $\begin{cases} \hat{I}: \quad \times \\ \widehat{M}_{xy}: \quad \checkmark \end{cases}$	Case 2a: $\begin{cases} \hat{I}: \quad \times \\ \widehat{M}_{xy}: \quad \times \\ \widehat{M}_{xy}S_+ = S_- \end{cases}$	Case 2b: $\begin{cases} \hat{I}: \quad \times \\ \widehat{M}_{xy}: \quad \times \\ \widehat{M}_{xy}S_+ = S_- \end{cases}$